Ecological Indicators 84 (2018) 450–458

Contents lists available at ScienceDirect

Ecological Indicators

journal homepage: www.elsevier.com/locate/ecolind

Technical note

El Niño Southern Oscillation cycle indicator for modeling extreme rainfall intensity over India

V. Agilan*, N.V. Umamahesh

Department of Civil Engineering, National Institute of Technology, Warangal, Telangana, 506004, India

ARTICLE INFO

Keywords:
ENSO cycle
ENSO cycle indicators
Extreme rainfall
India
Linear relationship

ABSTRACT

Since the global climate change altering the characteristics of extreme rainfall events, modeling the behavior of extreme rainfall is becoming indispensable. Among various physical processes, the El Niño Southern Oscillation (ENSO) cycle is a significant process that can trigger occurrences of extreme hydro-climatological events, such as floods, droughts and cyclones. Consequently, modeling the relationship between ENSO cycle and regional climate anomaly is gaining more attention in recent years. Studies in literature used various ENSO indices to quantify ENSO cycle in the statistical models which aim to model/forecast extreme rainfall and fail to report the best ENSO index for modeling extreme rainfall over India. Hence, this study is carried out to answer two research questions: (1) What is the best ENSO index for modeling extreme rainfall intensity over India? (2) What is the significance of identifying the best ENSO indicator for modeling extreme rainfall intensity over India? Towards answering these questions, the change in the linear relationship between ENSO cycle and extreme rainfall over India due to the choice of ENSO cycle indicator is examined. Results of this study indicate that the ENSO index Southern Oscillation Index (SOI) is the best ENSO index for modeling extreme rainfall over India. The results also show a significant change in ENSO-Extreme rainfall relationship due to the choice of ENSO index. In particular, 42% is the average increase in correlation coefficient between monsoon season extreme rainfall and ENSO cycle when the best ENSO index is chosen instead of the second-best ENSO index and it is around 37% for the non-monsoon season.

1. Introduction

In recent years, the extreme rainfall events are intensifying due to global climate change (Allen and Ingram, 2002; Emori and Brown, 2005; Trenberth et al., 2003; Xu et al., 2015; Cavanaugh et al., 2015). Since the extreme rainfall affects society significantly, it is inevitable to understand and analyze changes in them. In connection to that, the global research community tries to understand and quantify the relationship between regional climate anomaly and large-scale circulation. Among many large-scale circulations which cause changes in climate, the influence of the El Niño Southern Oscillation (ENSO) cycle on climate has drawn much attention in recent years (Geethalakshmi et al., 2009; Kenyon and Hegerl, 2010; Zhang et al., 2010; Zhang et al., 2013; Bothale and Katpatal, 2015). Because, the frequency of El Niño events (part of ENSO cycle) is increasing due to greenhouse warming (Timmermann et al., 1999; Cai et al., 2014). The temperature fluctuations between the atmosphere and the ocean in the east-central Equatorial Pacific is normally referred as the ENSO cycle (Zelle et al., 2004; Shi and Wang, 2014). The warm phase of the ENSO cycle is referred as El Niño and its counterpart is referred as La Niña. These phases of the ENSO cycle can have large-scale impacts on global weather and climate (Diaz et al., 2001; Zelle et al., 2004; Wu, 2016; Robinson et al., 2008; Agilan and Umamahesh, 2017). Further, this coupled ocean-atmosphere phenomenon is attributed to global climate variability on inter-annual time scales and occurrences of extreme hydro-climatological events, such as floods, droughts and cyclones (Zhang et al., 2007). Consequently, modeling the relationship between ENSO cycle and regional climate anomaly is gaining more attention.

The statistical models which aim to model/forecast rainfall use indices which characterize the ENSO cycle. Since the ENSO cycle is multifaceted and it involves different aspects of the atmosphere and the ocean over the tropical Pacific, several indices are used to represent the ENSO cycle, such as Southern Oscillation Index (SOI), Multivariate ENSO Index (MEI) and Sea Surface Temperature (SST). The ENSO index MEI is based on six main observed variables over the tropical Pacific Ocean. SOI is the sea level pressure differences between Tahiti and Darwin, Australia. The ENSO index SST is the sea surface temperature anomaly over the Pacific Ocean. In literature, the impact of ENSO cycle

* Corresponding author.
E-mail addresses: agilanvensiv@gmail.com (V. Agilan), mahesh@nitw.ac.in (N.V. Umamahesh).

http://dx.doi.org/10.1016/j.ecolind.2017.09.012
Received 23 February 2017; Received in revised form 1 September 2017; Accepted 7 September 2017
Available online 17 September 2017
1470-160X/

on Indian rainfall is mostly demonstrated with any of these three ENSO indices. For example, Singh (2001) used MEI as ENSO cycle indicator for analyzing the relationship between Indian monsoon rainfall and the ENSO cycle. Gadgil et al. (2004) analyzed the relationship between the extremes of the Indian summer monsoon rainfall and ENSO using SST. Rajeevan et al. (2008) and Revadekar and Kulkarni (2008) showed the possible relationship between extreme rainfall frequency over India and SST. Further, Revadekar and Kulkarni (2008) found that the frequency and intensity of extreme rainfall over Southern India have a strong linear relationship with SST anomalies 4–6 months in advance. Geethalakshmi et al. (2009) demonstrated the impact of ENSO on the north-east monsoon rainfall of Tamil Nadu, India using SOI and SST. Dimri (2012) showed the relationship between SOI and Northwest India winter precipitation. Kumar et al. (2014) used both SOI and SST as ENSO cycle indicator for analyzing the trends of rainfall pattern over homogeneous monsoon regions of India. Rajagopalan and Molnar (2014) used SST as ENSO cycle indicator for forecasting of early and late season Indian monsoon rainfall and its extremes. Recently, Mondal and Mujumdar (2015) used SST as ENSO cycle indicator for modeling the non-stationarity in the extreme daily rainfall characteristics over India. Bothale and Katpatal (2015) analyzed the influence of El Niño and La Niña (Parts of ENSO cycle) on trends and anomalies in extreme climate indices over Godavari Basin, India using the Oceanic Niño Index (ONI). The ONI is three months running mean of the SST anomalies in the Niño 3.4 region (refer Section 2.2) and it is mostly used to identify El Niño and La Niña years (Agilan and Umamahesh, 2015b; Bothale and Katpatal, 2015). Agilan and Umamahesh (2015b) analyzed the influence of El Niño and La Niña on the extreme rainfall events of Hyderabad city, India using ONI.

Though these studies were conducted over India and aim to find the relationship between ENSO cycle and Indian rainfall, they have not followed a single ENSO cycle indicator. In addition, some studies considered lag in the ENSO index while some of them have not. Therefore, it is not clear that which ENSO index is the best for Indian region. Maybe it will be the first question to researchers who are trying to find the ENSO effects on Indian rainfall. Hence, this study is carried out with two objectives: (1) identifying the best ENSO indicator for modeling extreme rainfall intensity over India; (2) demonstrating the significance of identifying the best ENSO indicator for modeling extreme rainfall intensity over India.

2. Data and methods

2.1. Rainfall

For this study, high-resolution gridded (1° Longitude × 1° Latitude) daily rainfall data prepared with the help of more than 1800 gauge observation over India is used and is available for the period of 1901–2004 (Rajeevan et al., 2008). This data set is prepared by India Meteorological Department (IMD) and the details about the preparation of this dataset can be obtained from Rajeevan et al. (2008). This dataset is increasingly being used in studies on Indian rainfall (Kulkarni et al., 2012; Mondal and Mujumdar, 2015).

2.2. ENSO indices

For this study, the ENSO cycle is represented by Southern Oscillation Index (SOI), Multivariate ENSO Index (MEI) and Sea Surface Temperature (SST). The monthly sea surface temperature anomaly (based on 1981–2010 mean) over NINO 3.4 (17°E-120°W, 5°S-5°N) region is used as SST index and it is available at http://www.esrl.noaa.gov/psd/gcos_wgsp/Timeseries/Data/nino34.long.anom.data (Accessed on 8th Jan 2017) The SOI is based on the difference in surface air pressure between Tahiti and Darwin and it is available at http://www.bom.gov.au/climate/current/soihtm1.shtml (Accessed on 8th Jan 2017). Compare to other ENSO indices, the ENSO index MEI incorporates more information and it is not affected by occasional data glitches in the monthly update cycles (Wolter and Timlin, 1998). The MEI is based on six main observed variables over the tropical Pacific i.e. sea-level pressure, zonal and meridional components of the surface wind, sea surface temperature, surface air temperature, and total cloudiness fraction of the sky. The ENSO index MEI is available at http://www.esrl.noaa.gov/psd/enso/mei.ext/table.ext.html (Accessed on 8th Jan 2017) The ENSO indicators i.e. MEI, SOI and SST are downloaded for the period of 1900–2004 (105 years).

2.3. Methods

2.3.1. Extracting extreme rainfall series

Rainfall during the four-month period of June through September is normally termed as the Indian summer monsoon season (Geethalakshmi et al., 2009; Kulkarni et al., 2012) and it receives around 76% of the total rainfall of India. Therefore, the best ENSO index is analyzed for monsoon and non-monsoon season separately. In the climate literature, the word “extreme” denote different things and there is no single definition for extreme (Stephenson, 2008; Agilan and Umamahesh, 2015a). However, an extreme can be reasonably well defined for any climate variable (such as rainfall) by referring to values in the tails of the distribution that would be expected to occur infrequently (Zeng and Zwires, 2013). For this study, the extreme rainfall is defined by different threshold values. First, the rainfall amount in rainy days is fitted with empirical Cumulative Distribution Function (CDF) and different percentile extreme rainfall are calculated from the empirical CDF. Then the extreme rainfall series are extracted using a threshold of different percentile rainfall in the peaks over threshold approach. In particular, for monsoon season, five extreme rainfall series are extracted using five threshold values, i.e. 90^{th}, 92.5^{th}, 95^{th}, 97.5^{th} and 99^{th} percentile monsoon extreme rainfall. Since the number of rainy days in a non-monsoon season of India is less when compared to the monsoon season rainy days, the 99^{th} percentile extreme rainfall of non-monsoon season will have very less rainy days (less than 10) for many grid points of India and it will have mostly insignificant correlation with the ENSO cycle. Consequently, only four extreme rainfall series are extracted from the non-monsoon rainfall series (corresponding to 90^{th}, 92.5^{th}, 95^{th} and 97.5^{th} percentile non-monsoon rainfall). The empirical CDF for monsoon seasons' rainfall values of a random grid point [Longitude = 68.5° E; Latitude = 23.5N°] is shown in Fig. 1 along with the calculated threshold values (corresponding to 90^{th}, 92.5^{th}, 95^{th}, 97.5^{th} and 99^{th} percentiles).

2.3.2. Identifying the best ENSO indicator

Towards identifying the best ENSO index, the linear relationship between extreme rainfall over India and different ENSO indices is studied. In details, the Pearson product-moment correlation coefficient (generally used to study the linear relationship between two variables) between different ENSO indices and monsoon and non-monsoon season extreme rainfall over India is analyzed for the period of 1901–2004. Once the extreme rainfall series are extracted, the linear relationship between extreme rainfall and ENSO indices can be obtained. Further, since some of the previous studies considered the lag in ENSO index, we also considered lag up to twelve months in each index. In details, first, the best ENSO index is selected for each lag value, then, the best ENSO index regardless of lag value is also identified.

After extracting extreme rainfall series which exceeds the threshold of ‘x’ percentile rainfall of the monsoon/non-monsoon season, the Pearson product-moment correlation coefficient (absolute value) is calculated between ‘x’ percentile extreme rainfall series of the selected season and three ENSO indices (i.e. MEI, SOI and SST) for a fixed lag-value (say 2 months). Among three ENSO indices, the ENSO index which has the maximum absolute correlation coefficient is considered as the best ENSO index for the particular grid (say grid 1), particular season (say monsoon), particular lag (say 2 months) and particular

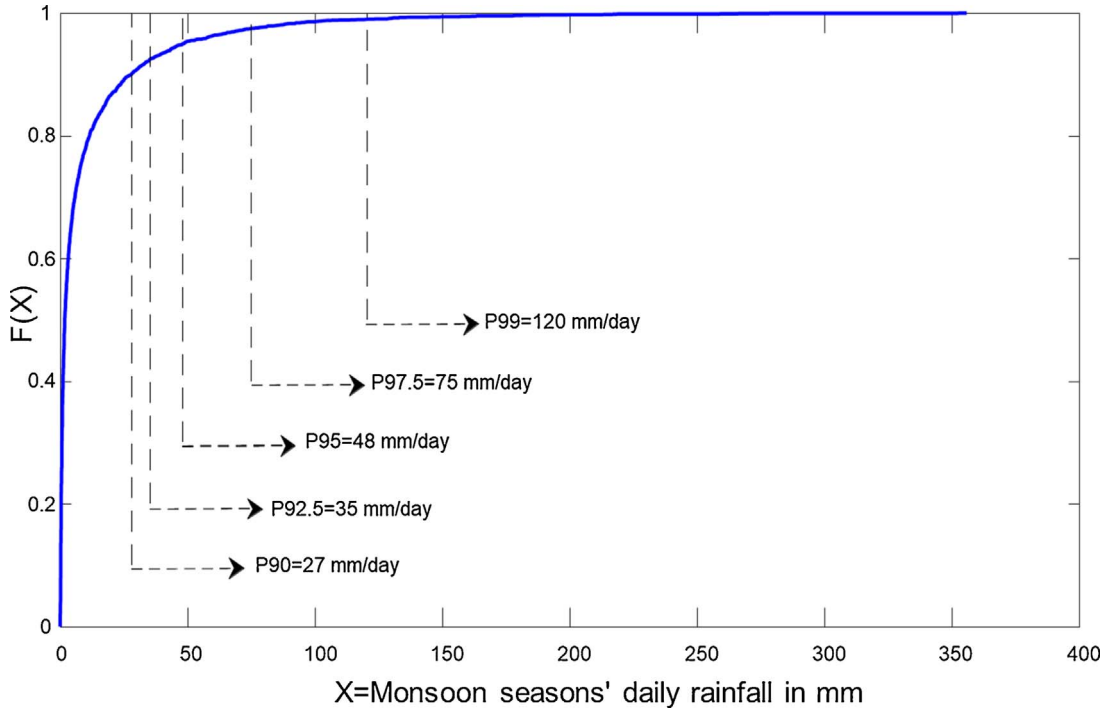

Fig. 1. The empirical Cumulative Distribution Function (CDF) for monsoon seasons' rainfall values of a random grid point [Longitude = 68.5°E; Latitude = 23.5N°] along with the calculated threshold values (corresponding to 90th, 92.5th, 95th, 97.5th and 99th percentiles). F(X) = cumulative relative frequencies of rainfall (e.g. P90 = 27 mm/day: 90% of all rainfall events had less or equal 27 mm rain/day).

percentile (say 95th) extreme rainfall series. In a similar manner, the best ENSO index for all grids, all seasons, all lag values and all percentile extreme rainfall series are identified.

Since the ENSO indices are based on different variables, some index may qualify as the best index in one lag while some other index may be the best index in the majority of lag values. Moreover, the lag at which ENSO cycle has an influence on Indian region extreme rainfall is not reported till date. Therefore, the best ENSO index for each grid, each season and each percentile extreme rainfall series is further analyzed regardless of the lag value in ENSO index. In details, first, the Pearson product-moment correlation coefficient (absolute value) is calculated between 'x' percentile extreme rainfall of a season and three ENSO indices (i.e. MEI, SOI and SST) with all lag values (i.e. 0–12 months). Then, the ENSO index which has the maximum absolute Pearson product-moment correlation coefficient (regardless of lag) is considered as the best ENSO index for the particular grid (say grid 1), particular season (say monsoon) and particular percentile (say 95th) extreme rainfall. Similarly, the best ENSO index for all grids, all seasons and all percentile extreme rainfall is identified regardless of the lag value in ENSO index.

2.3.3. Significance of the best ENSO indicator

The basic aim of this study is to identify the best ENSO index for modeling extreme rainfall over India. However, what is the significance of identifying the best ENSO index? Will the choice of ENSO index create a significant difference in modeling accuracy? To answer these questions, the percentage change in the Pearson product-moment correlation coefficient (absolute value) due to the choice of ENSO index is also analyzed.

3. Results and discussion

As stated earlier, in the direction of identifying the best ENSO indicator for each lag value (in months), the Pearson product-moment correlation coefficient (absolute value) is calculated between different percentile extreme rainfall series and three ENSO indices with a lag value up to 12 months. Firstly, for each lag value, the best ENSO index of each grid point for the given percentile monsoon extreme rainfall series is identified using the method described in Section 2.3. Then the number of grids (out of 357) at which the ENSO index is qualified as the best index is counted for all three ENSO indices and plotted in Fig. 2 for 90th, 92.5th, 95th, 97.5th and 99th percentile monsoon season extreme rainfall series. From Fig. 2, it is observed that the SOI is the best ENSO index for most of the grids and lag values. In other words, for most of the grids, the ENSO index SOI has the strongest linear relationship with monsoon season extreme rainfall series when compared to other ENSO indices.

Similar to monsoon season, for each lag value, the best ENSO index of each grid point for the given percentile non-monsoon extreme rainfall series is identified using the method described in Section 2.3. Then the number of grids (out of 357) at which the ENSO index is qualified as the best index is counted for all three ENSO indices and plotted in Fig. 3 for 90th, 92.5th, 95th and 97.5th percentile non-monsoon season extreme rainfall series. Like monsoon season, Fig. 3 shows that the SOI is the best ENSO indicator for modeling non-monsoon extreme rainfall series. Meaning, for most of the grids, the ENSO index SOI has the strongest linear relationship with non-monsoon season extreme rainfall series when compared to other ENSO indices.

The best ENSO indicator, regardless of lag value, for modeling monsoon season extreme rainfall over India is identified using the method described in Section 2.3 and presented as Circos diagram in Fig. 4. The Circos diagram uses a circular ideogram layout to facilitate the display of the relationships between a pair of variables represented by their position on a circle, and using ribbons or chords. From Fig. 4, it is noted that the ENSO index SOI is having a strongest linear relationship with different percentile monsoon season extreme rainfall of India. In particular, Circos diagram shows that the ENSO index SOI is the best ENSO index for modeling monsoon season extreme rainfall of more than 70% of grids (total number of grids = 357) of India. The other two ENSO indices share the remaining 30% of grids equally. Circos diagram also indicates that the best ENSO index is not changing significantly with respect to extreme rainfall threshold value (i.e. P90 to P99).

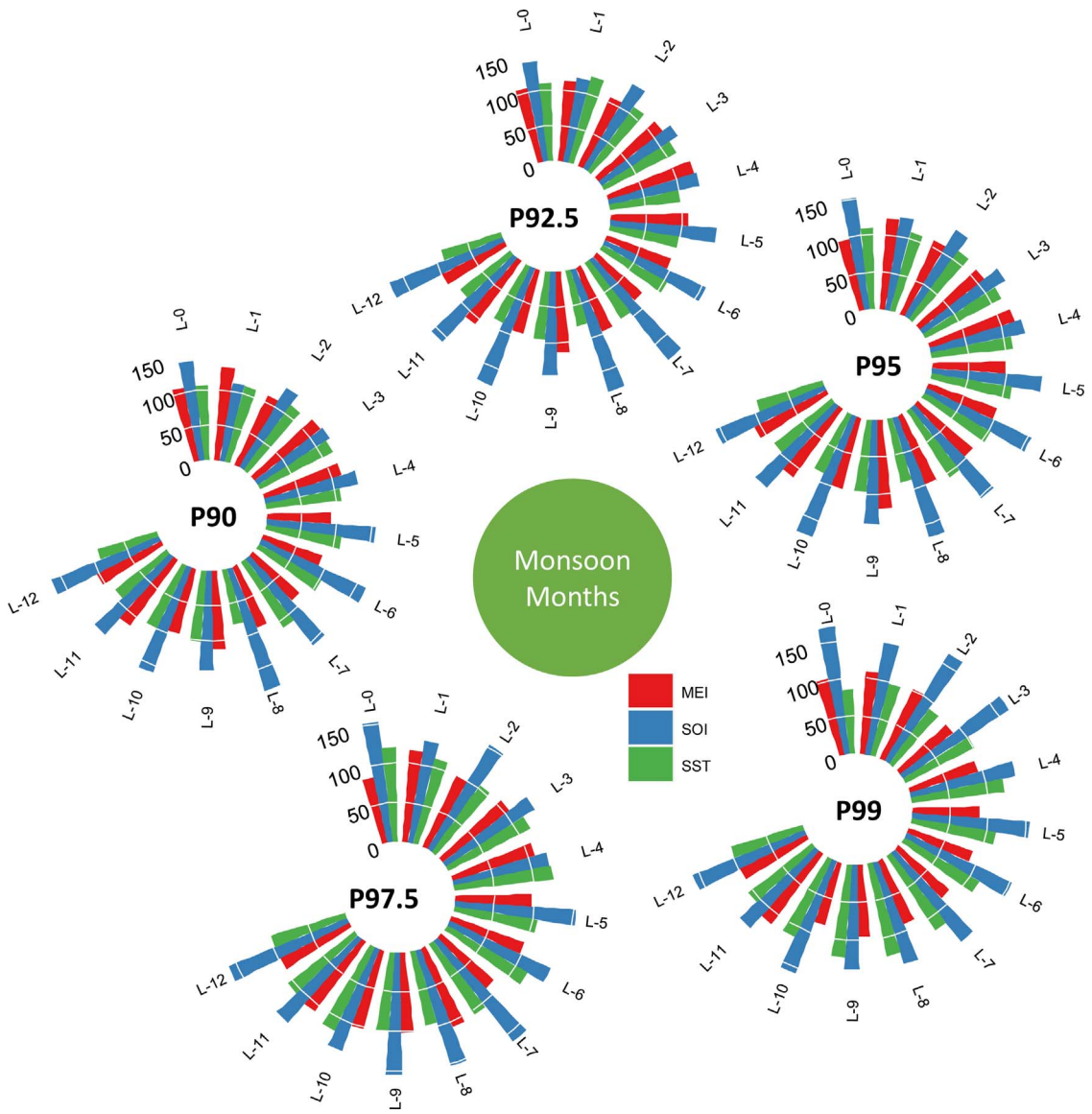

Fig. 2. The number of grids (out of 357) at which the ENSO indices (i.e. Southern Oscillation Index (SOI), Multivariate ENSO Index (MEI) and Sea Surface Temperature (SST)) qualified as the best ENSO index for 90th, 92.5th, 95th, 97.5th and 99th percentile monsoon extreme rainfall series. L-0, L-1,…,L-12 indicates zero month lag, one month lag, …, 12 months lag respectively. The ordinate indicates number of grids. The method for the identification of the best ENSO index is presented in Section 2.3.2.

Moreover, distributions of the best ENSO indices remain same across different percentile extreme rainfall series. The best ENSO indicator, regardless of lag value, for modeling non-monsoon season extreme rainfall over India is plotted in Fig. 5. Similar to monsoon season, from Fig. 5, it is observed that the ENSO index SOI has the strongest linear relationship with different percentile non-monsoon season extreme rainfall of India. In details, the ENSO index SOI is the best ENSO index for modeling non-monsoon season extreme rainfall of more than 65% of grids (total number of grids = 357) of India.

From the study results, it is noted that the ENSO index SOI is the best ENSO cycle indicator for modeling both monsoon and non-monsoon seasons' extreme rainfall intensity over India. However, if the study area is only part of India (ex. any city or region), SOI may not be the best ENSO cycle indicator. Henceforth, it is suggested to consider all ENSO indicators and select the best one, if the study focuses on some part of India. As aforementioned, this study basically aims to find the best ENSO index for modeling extreme rainfall over India. But, what is the significance of identifying the best ENSO index with appropriate lag? We explore this question through analyzing the percentage change in the linear relationship (absolute value of the Pearson product-moment correlation coefficient) due to the choice of ENSO index.

For example, the absolute value of the Pearson product-moment correlation coefficient between three ENSO indices (i.e. MEI, SOI and SST) and monsoon season 99th percentile extreme rainfall series of a random grid point [68.5° E and 23.5N°] is plotted in Fig. 6. Fig. 6 shows that the SOI with 4-month lag is the best ENSO cycle index for this grid point's monsoon season 99th percentile extreme rainfall series and it produced an absolute correlation coefficient of 0.40 (p-value = 0.01). Further, the second-best ENSO index for the same grid point is MEI with 12-months lag and it produced an absolute correlation coefficient of 0.21 (p-value: 0.21). In this case, it is worth to note that 0.40 is around 90% (refer Eq. (1)) higher than 0.21. In addition, the statistical significance of the correlation is changed from significant to insignificant. Furthermore, the third-best ENSO index for the selected random grid point is SST with 4-months lag and it produced an absolute correlation coefficient of 0.08 (p-value 0.65). Note that the absolute correlation coefficient produced with the best ENSO index of the grid point is around 400% higher than the absolute correlation coefficient produced with the third-best ENSO index of the grid point and the correlation coefficients calculated using the second-best and third-best ENSO

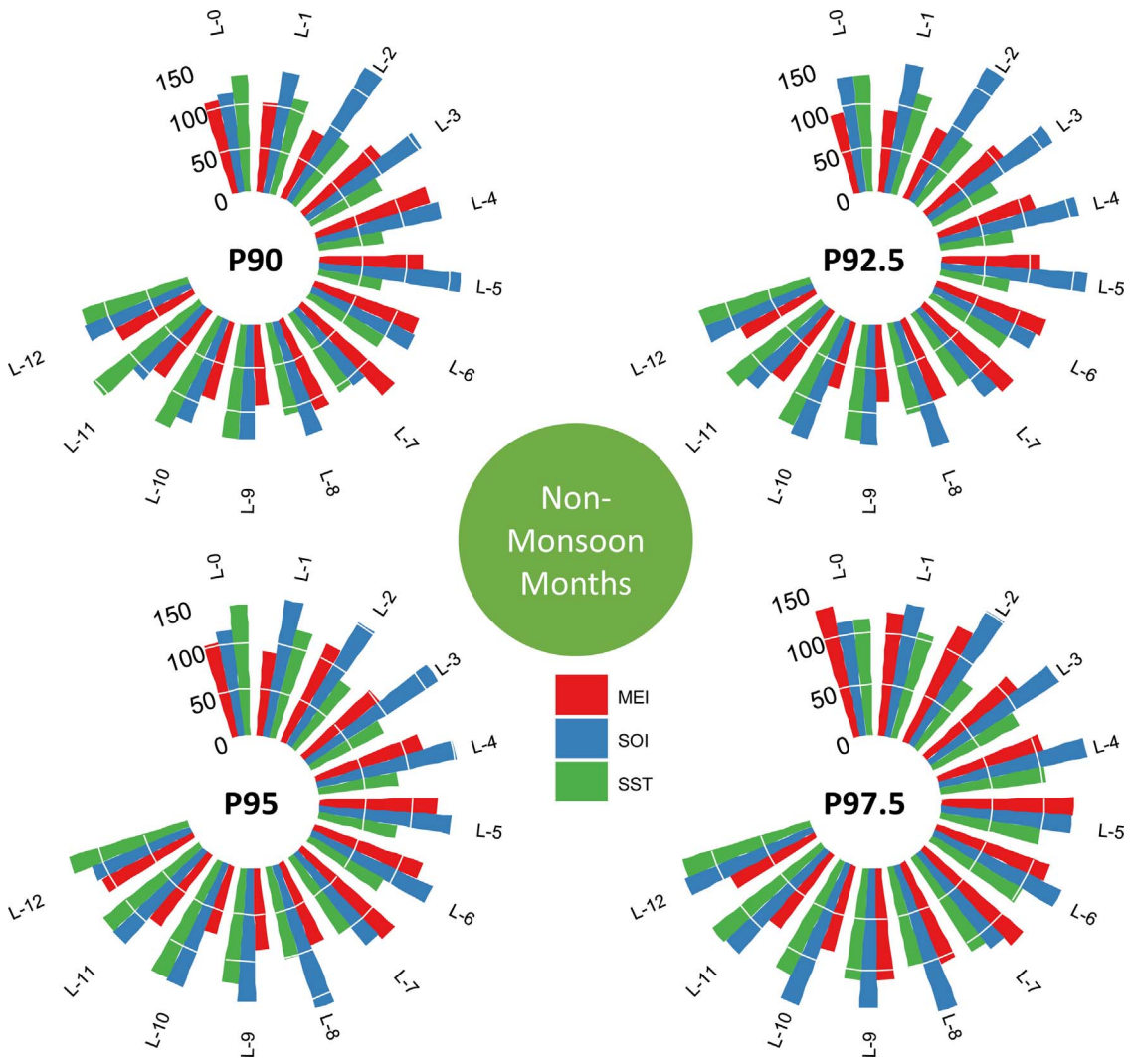

Fig. 3. The number of grids (out of 357) at which the ENSO indices (i.e. MEI, SOI and SST) qualified as the best ENSO index for 90th, 92.5th, 95th and 97.5th percentile non-monsoon extreme rainfall series. Explanation of Fig. 2 applies also to this.

indices are statistically insignificant ($p > 0.05$). In other words, the accuracy of extreme rainfall modeling of this grid point would be significantly higher if the modeler uses SOI instead of SST or MEI for representing ENSO cycle in the statistical model. Further, to obtain the overall picture, the percentage change (Eq. (1)) in absolute correlation coefficient value between the best ENSO index and the second-best/third-best ENSO index is analyzed for all grid points' and all seasons' different percentile extreme rainfall series.

$$pc = 100 \times \left(\frac{|r_b| - |r_{b*}|}{|r_{b*}|} \right) \quad (1)$$

In Eq. (1), $|r_b|$ is the absolute correlation coefficient between the best ENSO index and the extreme rainfall series and $|r_{b*}|$ is the absolute correlation coefficient between the second-best/third-best ENSO index and the extreme rainfall series. The boxplots of the percentage change (Eq. (1)) in absolute correlation coefficient between the best and the second-best/third-best ENSO index is plotted in Fig. 7. Similar to the selected random grid point, a significant change in the absolute correlation coefficient value due to the choice of ENSO index is observed from Fig. 7. On an average, the absolute correlation coefficient calculated between monsoon season extreme rainfall and the best ENSO index of the grid is around 42% higher than the absolute correlation coefficient calculated between monsoon season extreme rainfall and the second-best ENSO index of the grid. Similarly, 37% is the average increase in correlation coefficient between non-monsoon season extreme rainfall and ENSO cycle when the best ENSO index is chosen instead of the second-best ENSO index for calculating the correlation coefficient. In addition, the average increase in the correlation coefficient between the best and the third-best ENSO index is 84% and 69% for monsoon and non-monsoon seasons respectively. Moreover, for many grid points, the statistical significance of correlation coefficient (at the significance level of 0.05) is changed from insignificant to significant when the best ENSO index is used instead of the second-best ENSO index. Hence, it is clear that the choice of ENSO index will make a significant difference in analyzing/modeling ENSO cycle impacts on Indian region extreme rainfall. Note that the percentage in correlation coefficient due to the choice of ENSO index is higher for monsoon season when compared to the non-monsoon season. In addition to these findings, from the results (not shown in this paper), we also observed that the correlation between ENSO and extreme rainfall is becoming stronger when the percentile (threshold) of monsoon/non-monsoon season extreme rainfall is increased. In other words, the very rare events of India are having a strong correlation with the ENSO cycle than rare events.

4. Summary and conclusions

Since the global climate change altering the characteristics (i.e.

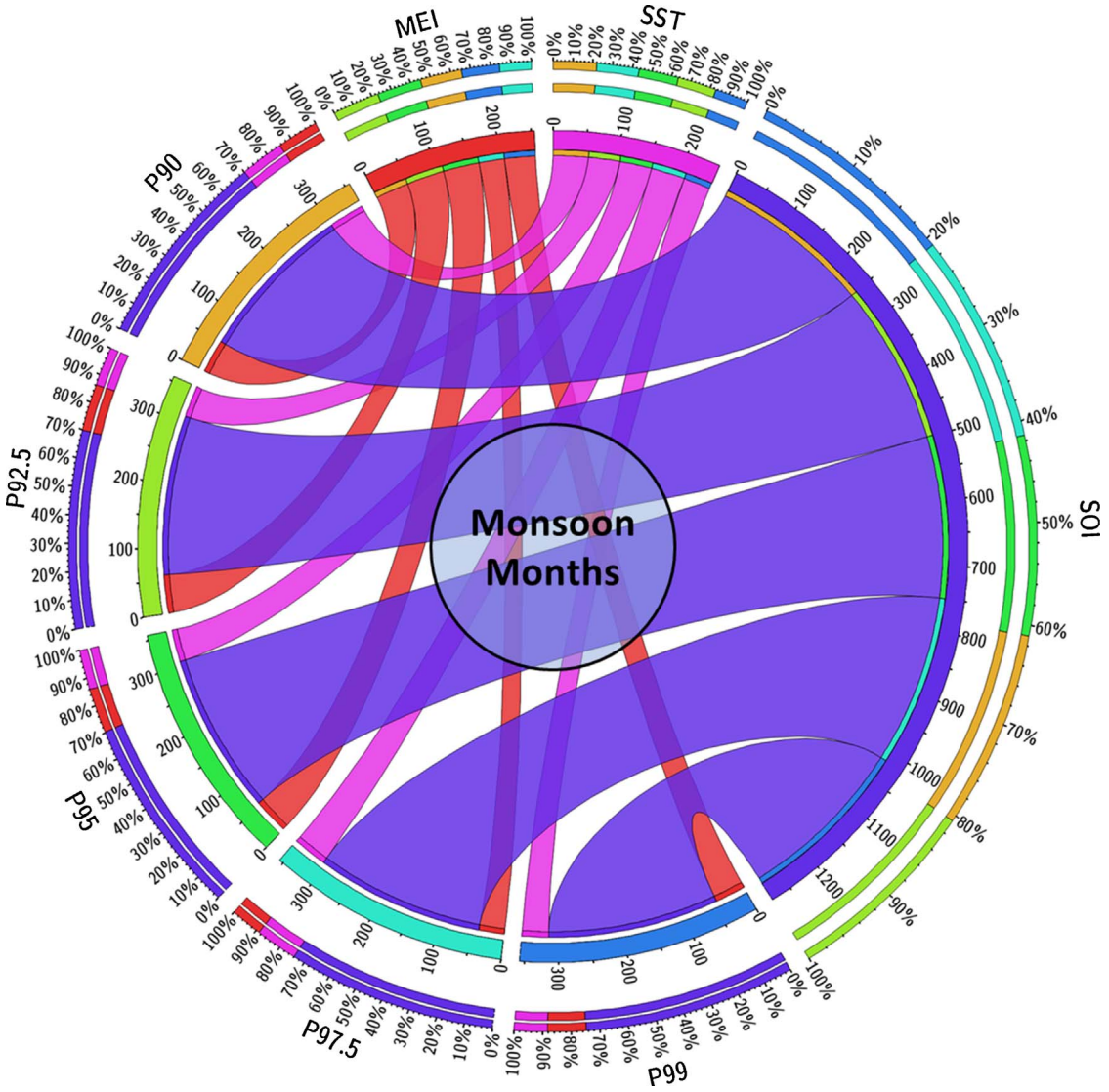

Fig. 4. Circos diagram shows the ENSO indicator for modeling monsoon season extreme rainfall over India. Purple, pink and orange colors in the Circos diagram indicate the ENSO indices SOI, SST and MEI respectively. Similarly, goldenrod, pale-green, apple-green, turquoise and blue colors in the Circos diagram indicate the extreme rainfall percentiles P90, P92.5, P95, P97.5 and P99 respectively. Values on the inner circle represent the number of grids while the values on the outer circle represent the percentage. (For interpretation of the references to colour in this figure legend, the reader is referred to the web version of this article.)

duration, frequency and intensity) of extreme rainfall events, modeling the behavior of extreme rainfall is becoming indispensable. Among various physical processes, the ENSO cycle is a significant process that can trigger occurrences of extreme hydro-climatological events, such as floods, droughts and cyclones. Moreover, the frequency of El Niño events is increasing due to greenhouse warming (Cai et al., 2014; Timmermann et al., 1999). Consequently, modeling the relationship between ENSO cycle and regional climate anomaly is gaining more attention in recent years. Studies in literature used various ENSO indices to quantify ENSO cycle in the statistical models which aim to model/forecast extreme rainfall and fail to report the best ENSO index for modeling extreme rainfall over India. Hence, this study is focused on answering two research questions: (1) What is the best ENSO index for modeling extreme rainfall intensity over India? (2) What is the significance of identifying the best ENSO indicator for modeling extreme rainfall intensity over India?

In this study, the best ENSO index is analyzed for monsoon and non-monsoon seasons separately. For each season, a number of extreme rainfall series are obtained by defining various percentile of extreme rainfall in the peaks over threshold approach. Then the best ENSO index is identified by analyzing the strength of linear relationship between different extreme rainfall series and various ENSO indices. Further, since some of the previous studies considered the lag in ENSO index, the best ENSO index is analyzed for each month lag (up to twelve months). In addition, the best ENSO index is analyzed regardless of the lag value in the ENSO index. From the study results, for most of the grids, it is observed that the ENSO index SOI has the strongest linear relationship with different percentile extreme rainfall (both monsoon and non-monsoon season) of India when compared to other ENSO indices. In details, the ENSO index SOI is the best ENSO index for modeling monsoon season extreme rainfall of more than 70% of grids (total number of grids = 357) of India and it is around 65% for the non-monsoon season.

Further, the significance of selecting the best ENSO index is analyzed by calculating the percentage change in the Pearson product-moment correlation coefficient (absolute value) due to the choice of ENSO index. The results show a significant change in the Pearson product-moment correlation coefficient value due to the choice of ENSO index. Particularly, on an average, the absolute correlation coefficient calculated between monsoon season extreme rainfall and the best ENSO index of the grid is around 42% higher than the absolute correlation coefficient calculated between monsoon season extreme

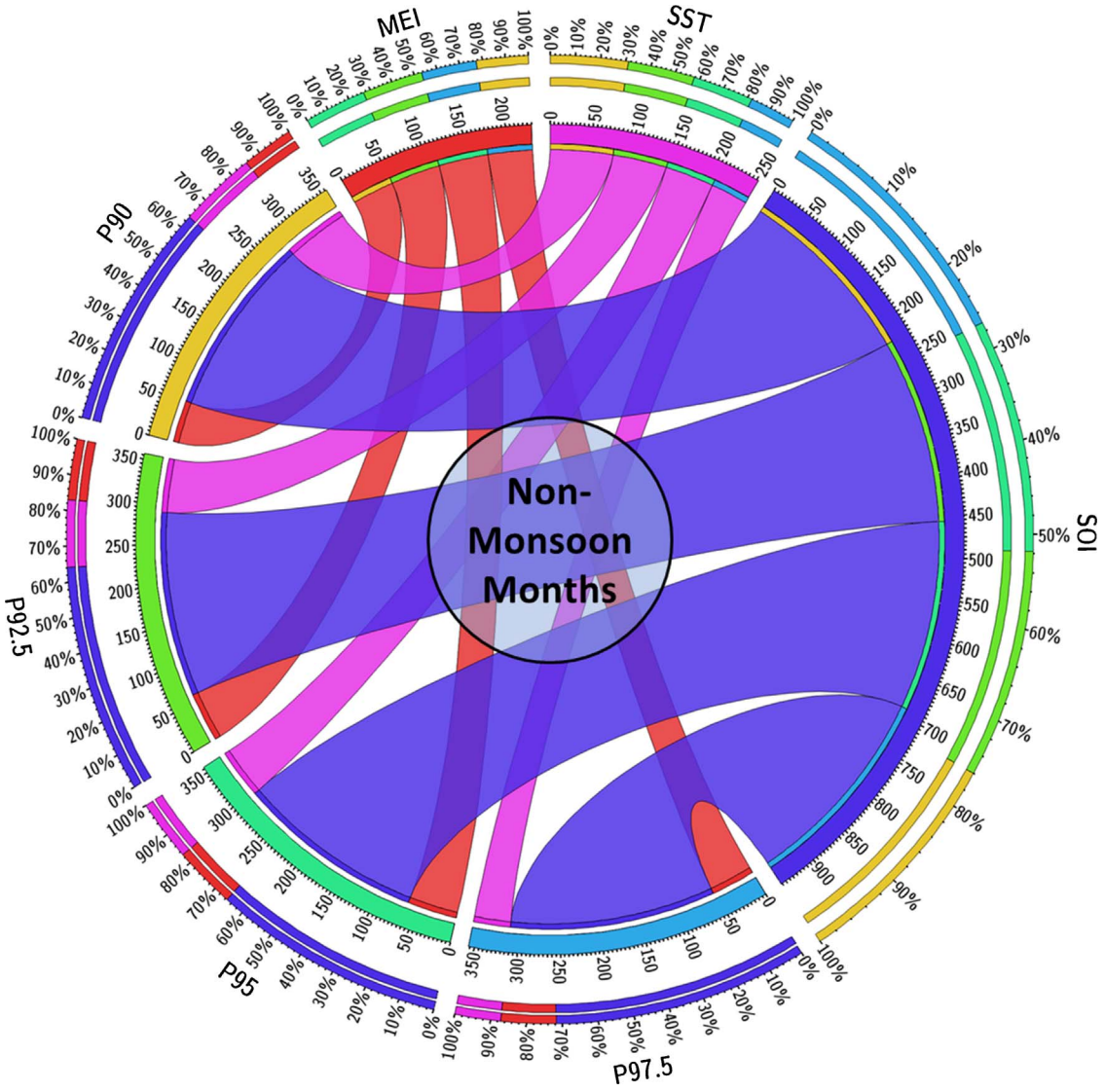

Fig. 5. Circos diagram shows the ENSO indicator for modeling non-monsoon season extreme rainfall over India. Purple, pink and orange colors in the Circos diagram indicate the ENSO indices SOI, SST and MEI respectively. Similarly, goldenrod, pale-green, apple-green and azure colors in the Circos diagram indicate the extreme rainfall percentiles P90, P92.5, P95 and P97.5 respectively. Values on the inner circle represent the number of grids while the values on the outer circle represent the percentage. (For interpretation of the references to colour in this figure legend, the reader is referred to the web version of this article.)

rainfall and the second-best ENSO index of the grid. Similarly, 37% is the average increase in correlation coefficient between non-monsoon season extreme rainfall and ENSO cycle when the best ENSO index is chosen instead of the second-best ENSO index for calculating the correlation coefficient. In addition, the average increase in the correlation coefficient between the best and the third-best ENSO index is 84% and 69% for monsoon and non-monsoon seasons respectively. Note that the percentage in correlation coefficient due to the choice of ENSO index is higher for monsoon season when compared to the non-monsoon season. The findings of this study are useful for statistical models which focus

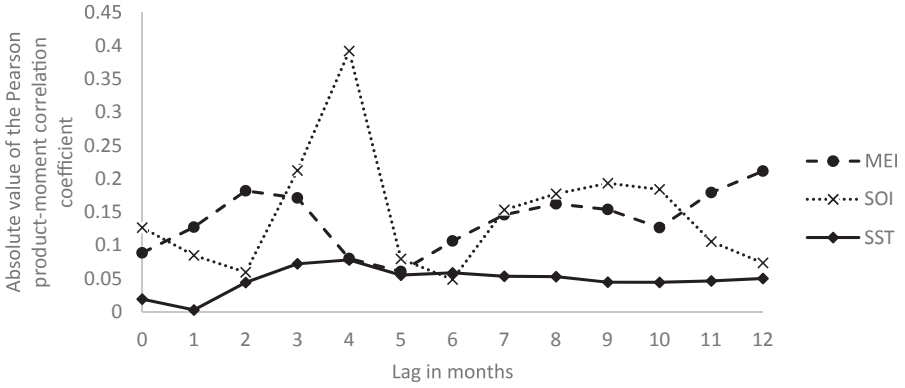

Fig. 6. Absolute value of the Pearson product-moment correlation coefficient between three ENSO indices (i.e. MEI, SOI and SST) and monsoon season's 99th percentile extreme rainfall series of a random grid point [Longitude = 68.5°E; Latitude = 23.5N°]. The monsoon season's 99th percentile extreme rainfall of this grid is 120 mm and there are 36 rainy days exceeds this value. The absolute correlation coefficient between 99th percentile extreme rainfall series of this grid and the ENSO index SOI with four months lag is 0.40 (p-value = 0.01). If the rainfall in August (say the year 1991) month exceeds the threshold (120 mm), the lag-0 correlation is calculated using August (same year) month's ENSO index value; the lag-1 correlation is calculated using July (same year) month's ENSO index value and so on.

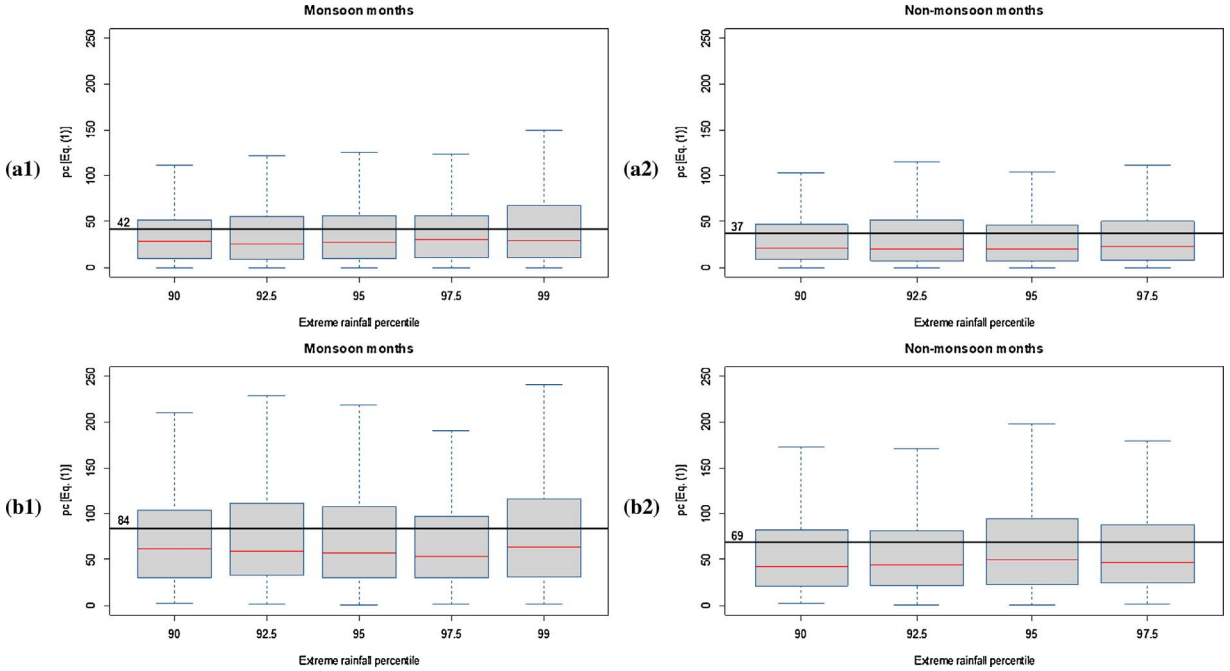

Fig. 7. The percentage change in the absolute correlation coefficients between (a) the best ENSO index and the second-best index, (b) the best ENSO index and the third-best index, for the monsoon months (1) and the non-monsoon months (2). Each box plot represents a frequency distribution with a median and the 25 and 75% percentiles, the extremes are given by vertical lines (whisker 2.5% and 97.5%). Ordinates = Change of absolute correlation coefficient (in%). Black horizontal line shows the mean value (across the rainfall percentiles).

on forecasting Indian extreme rainfall, modeling non-stationarity in Indian extreme rainfall and studies relating ENSO cycle and Indian extreme rainfall. Further, a similar study can be carried to find the best ENSO index for modeling extreme rainfall of other parts of the world. In addition, results of this study open another research question i.e. Why the SOI is the best ENSO index for modeling extreme rainfall over India? Answering this question by modeling the physical linkage would be a possible future work.

Acknowledgements

This work is supported by the Information Technology Research Academy (ITRA), Government of India under, ITRA-water grant ITRA/15(68)/water/IUFM/01. We also thank the India Meteorological Department for providing rainfall data. We also thank the editor and three anonymous reviewers whose constructive comments helped to improve the manuscript's clarity and quality.

References

Agilan, V., Umamahesh, N.V., 2015a. Detection and attribution of non-stationarity in intensity and frequency of daily and 4-h extreme rainfall of Hyderabad, India. J. Hydrol. 530, 677–697.
Agilan, V., Umamahesh, N.V., 2015b. Effect of el Niño-southern oscillation (ENSO) cycle on extreme rainfall events of Indian urban area. In: Proceedings of International Conference on Sustainable Energy and Built Environment. Vellore. pp. 569–573.
Agilan, V., Umamahesh, N.V., 2017. What are the best covariates for developing non-stationary rainfall intensity-duration-frequency relationship? Adv. Water Resour. 101, 11–22.
Allen, M.R., Ingram, W.J., 2002. Constraints on future changes in climate and the hydrologic cycle. Nature 419, 224–232.
Bothale, R.V., Katpatal, Y.B., 2015. Trends and Ānomalies in extreme climate indices and influence of El Ni˜no and La Ni˜na over pranhita catchment in Godavari basin, India. J. Hydrologic Eng pp. 05015023-1-12.
Cai, W., Borlace, S., Lengaigne, M., Van Rensch, P., Collins, M., Vecchi, G., Timmermann, A., Santoso, A., McPhaden, M.J., Wu, L., England, M.H., 2014. Increasing frequency of extreme El Niño events due to greenhouse warming. Nat. Clim. Change 4, 111–116.
Cavanaugh, N.R., Gershunov, A., Panorska, A.K., Kozubowski, T.J., 2015. The probability distribution of intense daily precipitation. Geophys. Res. Lett. 42.
Diaz, H.F., Hoerling, M.P., Eischeid, J.K., 2001. ENSO variability, teleconnections and climate change. Int. J. Climatol. 21 (15), 1845–1862.
Dimri, A.P., 2012. Relationship between ENSO phases with Northwest India winter precipitation. Int. J. Climatol. 33 (8), 1917–1923.
Emori, S., Brown, S.J., 2005. Dynamic and thermodynamic changes in mean and extreme precipitation under changed climate. Geophys. Res. Lett. 35, L17706.
Gadgil, S., Vinayachandran, P.N., Francis, P.A., Gadgil, S., 2004. Extremes of the Indian summer monsoon rainfall, ENSO and equatorial Indian Ocean oscillation. Geophys. Res. Lett. 31 pp. L12213:1-4.
Geethalakshmi, V., Yatagai, A., Palanisamy, K., Umetsu, C., 2009. Impact of ENSO and the Indian Ocean Dipole on the north-east monsoon rainfall of Tamil Nadu State in India. Hydrol. Process. 23, 633–647.
Kenyon, J., Hegerl, G.C., 2010. Influence of modes of climate variability on global precipitation extremes. J. Climate 23 (23), 6248–6262.
Kulkarni, M.A., Singh, A., Mohanty, U.C., 2012. Effect of spatial correlation on regional trends in rain events over India. Theor. Appl. Climatol. 109, 497–505.
Kumar, T.L., Rao, K.K., Barbosa, H., Uma, R., 2014. Trends and extreme value analysis of rainfall pattern over homogeneous monsoon regions of India. Nat. Hazards 73 (2).
Mondal, A., Mujumdar, P.P., 2015. Modeling non-stationarity in intensity, duration and frequency of extreme rainfall over India. J. Hydrol. 521, 217–231.
Rajagopalan, B., Molnar, P., 2014. Combining regional moist static energy and ENSO for forecasting of early and late season Indian monsoon rainfall and its extremes. Geophys. Res. Lett. 41 (12), 4323–4331.
Rajeevan, M., Bhate, J., Jaswal, A.K., 2008. Analysis of variability and trends of extreme rainfall events over India using 104 years of gridded daily rainfall data. Geophys. Res. Lett. 35 pp. L18707:1-6.
Revadekar, J.V., Kulkarni, A., 2008. The El Nino-Southern Oscillation and winter precipitation extremes over India. Int. J. Climatol. 28, 1445–1452.
Robinson, L.F., de la Pena, V.H., Kushnir, Y., 2008. Detecting shifts in correlation and variability with application to ENSO-monsoon rainfall relationships. Theor. Appl. Climatol. 94, 215–224.
Shi, W., Wang, M., 2014. Satellite-observed biological variability in the equatorial Pacific during the 2009–2011 ENSO cycle. Adv. Space Res. 54, 1913–1923.
Singh, O.P., 2001. Multivariate ENSO index and Indian monsoon rainfall: relationships on monthly and subdivisional scales. Meteorol. Atmos. Phys. 78, 1–9.
Stephenson, D.B., 2008. Definition, diagnosis, and origin of extreme weather and climate events. Climate Extremes and Society. Cambridge University Press, Cambridge.
Timmermann, A., et al., 1999. Increased El NinÃo frequency in a climate model forced by future greenhouse warming. Nature 398, 694–697.
Trenberth, K.E., Dai, A., Rasmussen, R.M., Parsons, D.B., 2003. The changing character of precipitation. Bull. Am. Meteorol. Soc. 84 (9), 1205–1217.
Wolter, K., Timlin, M.S., 1998. Measuring the strength of ENSO events: how does 1997/98 rank? Weather 53 (9), 315–324.
Wu, R., 2016. Possible roles of regional SST anomalies in long-term changes in the relationship between the Indian and Australian summer monsoon rainfall. Theor. Appl. Climatol. 124 (3–4), 663–677.
Xu, L., Zhou, H., Du, L., Yao, H., Wang, H., 2015. Precipitation trends and variability from 1950 to 2000 in arid lands of Central Asia. J. Arid Land 7 (4), 514–526.
Zelle, H., Appeldoorn, G., Burgers, G., Oldenborgh, G.J., 2004. The relationship between sea surface temperature and thermocline depth in the eastern equatorial pacific. J. Phys. Oceanogr. 34, 643–655.
Zeng, X., Zwires, F.W., 2013. Statistical indices for the diagnosing and detecting changes

in extremes. Extremes in a Changing Climate: Detection, Analysis and Uncertainty. Springer, pp. 1–14 s.l.
Zhang, Q., Xu, C., Jiang, T., Wu, Y., 2007. Possible influence of ENSO on annual maximum streamflow of the Yangtze River, China. J. Hydrol. 333, 265–274.
Zhang, X., Wang, J., Zwiers, F.W., 2010. The influence of large-scale climate variability on winter maximum daily precipitation over north America. J. Climate 23, 2902–2915.
Zhang, Q., Li, J., Singh, V.P., Xu, C.Y., Deng, J., 2013. Influence of ENSO on precipitation in the East River basin, south China. J. Geophys. Res.: Atmos. 118, 1–13.